

Mechanistics of Early Stage Growth of AlN on Alumina. 2. TMAI and NH₃

D. C. Bertolet, Herng Liu, and J. W. Rogers, Jr.*

Department of Chemical Engineering, BF-10, University of Washington,
Seattle, Washington 98195

Received June 25, 1993. Revised Manuscript Received October 1, 1993*

The reactions of trimethylaluminum (TMAI) and ammonia (NH₃) on γ -alumina were studied by Fourier transform infrared spectroscopy, thermal desorption spectroscopy, and X-ray photoelectron spectroscopy (XPS) to explore their feasibility as precursors for the low-temperature growth of AlN. Upon exposure of TMAI and NH₃, covalently bonded Al-N networks are formed at room temperature. This reaction efficiency is enhanced by a factor of 4 when the NH₃ is dosed with the substrate at 600 K. An atomic layer growth process involving cyclic processing at 600 K yielded site-specific reaction of the TMAI, followed by facile reaction of the ammonia to create new sites for the TMAI reaction. XPS results confirmed the presence of AlN.

Introduction

Because of the many important potential applications of AlN thin films, we¹ and others²⁻⁵ have carried out fundamental investigations of the low-temperature chemical vapor deposition of AlN. The interest in AlN is driven by its unique combination of material properties, which invite applications ranging from dielectric layers in high-temperature semiconductor structures, to microelectronics packaging,⁶ to surface acoustic wave devices,⁷ and potentially even optical devices operating in the blue region of the spectrum and beyond.⁸

One of the most promising methods of preparing AlN thin films is by metalorganic chemical vapor deposition (MOCVD). The MOCVD technique has many attractive features, including high deposition rates, the potential for depositing a wide variety of materials, the ability to form abrupt interfaces and deposit conformal coatings, and the relative simplicity of the apparatus.⁹ MOCVD of AlN thin films has been reported by several groups,¹⁰⁻¹⁶ but to

achieve epitaxial deposition, temperatures in the range of 1400 K and above typically have been required. Recently the epitaxial growth of AlN by "metalorganic surface chemical absorption deposition" at 673 K was reported.¹⁷ Deposition of AlN thin films at high temperature creates a major impediment to their use because many applications require substrates which cannot tolerate a high-temperature processing step.

The MOCVD process is quite complex, involving both homogeneous and heterogeneous reactions, and fundamental investigations of the inherent surface reaction mechanisms have been limited.^{18,19} Fewer still have studied the chemistry involved in AlN thin-film processing. Chemisorption of trimethylaluminum (TMAI) on silica has been reported by several groups,^{2,20-27} and the coadsorption of TMAI and NH₃ on silica³ and Si(100)⁴ has also been reported recently.

A variation of the CVD process, known as atomic layer growth, has been successfully applied to the deposition of various group III-V semiconductor materials by a number of laboratories.²⁸⁻³² Atomic layer growth offers the potential for low-temperature deposition, as well as precise control of layer thickness and interface abruptness. In general, atomic layer growth involves a two-step process in which alternating monolayers of materials are adsorbed

* Abstract published in *Advance ACS Abstracts*, November 15, 1993.

- (1) Bertolet, D. C.; Rogers, Jr., J. W. *Chem. Mater.* 1993, 5, 391.
- (2) Bartram, M. E.; Michalske, T. A.; Rogers, Jr., J. W. *J. Phys. Chem.* 1991, 95, 4453.
- (3) Bartram, M. E.; Michalske, T. A.; Rogers, Jr., J. W.; Mayer, T. M. *Chem. Mater.* 1991, 3, 953.
- (4) Mayer, T. M.; Rogers, Jr., J. W.; Michalske, T. A. *Chem. Mater.* 1991, 3, 641.
- (5) Interrante, L. V.; Sigel, G. A.; Garbaskas, M.; Hejna, C.; Slack, G. A. *Inorg. Chem.* 1989, 28, 252.
- (6) Tummala, R. R.; Rymaszewski, E. J. *Microelectronics Packaging Handbook*; Van Nostrand Reinhold: New York, 1989; p 36.
- (7) O'Toole, R. P.; Burns, S. G.; Porter, M. D.; Bastiaans, G. J. *Anal. Chem.* 1992, 64, 1289.
- (8) Strite, S.; Morkoc, H. *J. Vac. Sci. Technol. B* 1992, 10, 1237.
- (9) Stringfellow, G. B. *Organometallic Vapor-Phase Epitaxy: Theory and Practice*; Academic Press: New York, 1989; p 3.
- (10) Manasevit, H. M.; Erdmann, F. M.; Simpson, W. I. *J. Electrochem. Soc.* 1971, 118, 1864.
- (11) Morita, M.; Norihiko, U.; Isogai, S.; Tsubouchi, K.; Mikoshiba, N. *Jpn. J. Appl. Phys.* 1981, 20, 17.
- (12) Duffy, M. T.; Wang, C. C.; O'Clock, Jr., G. D.; McFarlane, III, S. H.; Zanzucchi, P. J. *J. Electron. Mater.* 1973, 2, 359.
- (13) Eichhorn, G.; Rensch, U. *Phys. Status Solidi* 1982, A69, K3.
- (14) Matloubian, M.; Gershenzon, M. J. *Electron. Mater.* 1985, 14, 633.
- (15) Rensch, U.; Eichhorn, G. *Phys. Status Solidi* 1983, A77, 195.
- (16) Chubachi, Y.; Sato, K.; Kojima, K. *Thin Solid Films* 1984, 122, 259.
- (17) Yu, Z. J.; Edgar, J. H.; Ahmed, A. U.; Rys, A. *J. Electrochem. Soc.* 1991, 138, 196.

- (18) Kuech, T. F. *Mater. Sci. Rep.* 1987, 2, 1.
- (19) Zanella, P.; Rossetto, G.; Brianese, N.; Ossola, F.; Porchia, M.; Williams, J. O. *Chem. Mater.* 1991, 3, 225.
- (20) Murray, J.; Sharp, M. J.; Hockey, J. A. *J. Catal.* 1970, 18, 52.
- (21) Yates, D. J. C.; Deinbinski, G. W.; Kroll, W. R.; Elliot, J. J. *J. Phys. Chem.* 1969, 73, 911.
- (22) Peglar, R. J.; Murray, J.; Hambleton, F. H.; Sharp, M. J.; Parker, A. J.; Hockey, J. A. *J. Chem. Soc. A* 1970, 2170.
- (23) Peglar, R. J.; Hambleton, F. H.; Hockey, J. A. *J. Catal.* 1971, 20, 309.
- (24) Kunawicz, J.; Jones, P.; Hockey, J. A. *Trans. Faraday Soc.* 1971, 67, 848.
- (25) Low, M. J. D.; Severdia, A. G.; Chan, J. *J. Catal.* 1981, 69, 384.
- (26) Kinney, J. B.; Staley, R. H. *J. Phys. Chem.* 1983, 87, 3735.
- (27) Morrow, B. A.; McFarlan, A. J. *J. Non-Cryst. Solids* 1990, 120, 61.
- (28) Aoyagi, Y.; Doi, A.; Iwai, S.; Namba, S. *J. Vac. Sci. Technol. B* 1987, 5, 1460.
- (29) DenBaars, S. F.; Dapkus, P. D. *J. Cryst. Growth* 1988, 93, 195.
- (30) Nishizawa, J.; Kurabayashi, T. *J. Cryst. Growth* 1988, 93, 98.
- (31) Tischler, M. A.; Bedair, S. M. *Appl. Phys. Lett.* 1986, 48, 1681.
- (32) Ozeki, M.; Mochizuki, K.; Ohtsuka, N. K. *Appl. Phys. Lett.* 1989, 53, 1509.

in sequential exposures of each precursor. Two aspects of the atomic layer growth process that appear to be essential are a self-limiting adsorption of one or both of the precursor gases^{29,30} and site-selective incorporation of components into the proper surface configuration.^{33,34} The first requirement leads to the incorporation of a single atomic layer per cycle and is accomplished by control of the adsorption or decomposition kinetics of the precursor. The second requirement leads to control of the stoichiometry and structure of the film. Group III–V compounds are ideal candidates for atomic layer growth because the decomposition of the group III alkyl precursors can be controlled at low temperatures to give self-limiting adsorption, and the complementary acid–base characteristics of the electron-deficient group III (Lewis acid) and electron-rich group V (Lewis base) components lead naturally to site-selective incorporation.

In a previous publication¹ we presented a Fourier-transform infrared (FTIR) study of the reactions of TMAI and NH_3 on alumina. Alumina was chosen as a substrate because (i) its surface chemistry is thought to be similar to that of a crystalline substrate, (ii) its high surface area makes it amenable to study by IR in the transmission mode, and (iii) it is transparent in the wavelength range of interest ($4000\text{--}1500\text{ cm}^{-1}$) allowing investigation of adsorbate features. We determined that TMAI reacts with hydroxyl groups on the alumina surface to form primarily a dimethylaluminum (Me_2Al) surface complex singly bound to oxygen. When this complex is subsequently exposed to ammonia at room temperature, a weakly bound $\text{Me}_2\text{Al:NH}_3$ adduct is formed, along with amide ($-\text{NH}_2-$) covalently bonded to aluminum. In the present paper, we describe further results with TMAI and NH_3 on alumina, including temperature-programmed desorption (TPD) studies, X-ray photoelectron spectroscopy (XPS) measurements, and the demonstration of an atomic layer growth process. The ongoing goal of this work is to understand the mechanistics of the surface reactions involved in MOCVD processing of AlN, and to find routes to lower the AlN processing temperatures.

Experimental Section

Deposition and infrared (IR) spectroscopy were performed in a stainless steel vacuum chamber with a base pressure of 1×10^{-8} Torr. The system was equipped with a turbomolecular pump, an ion pump, an ion gauge, a capacitance manometer, and a gas-handling manifold incorporating a leak valve and ballast. A schematic of the apparatus is shown in Figure 1. The chamber was mounted within the sample compartment of an FTIR system (Bruker Instruments, Inc., Model IR98, Billerica, MA) and is sealed from the external ambient by an O-ring. In this manner, the entire IR beam path could be evacuated. O-ring sealed, differentially pumped KBr windows were employed to pass the IR beam through the high-vacuum chamber, and the sample was moved in and out of the IR beam path with a bellows assembly. The IR data were recorded from 4000 to 1000 cm^{-1} with a resolution of 4 cm^{-1} , using a KBr beam splitter and a DTGS detector. For each spectrum, a new reference scan, with the sample out of the beam path, was taken to calculate absorbance and eliminate the effects of background changes (if any), such as deposition on the KBr windows. All of the FTIR spectra presented here were obtained by subtracting the spectrum of the clean alumina substrate from the spectrum taken after precursor exposure. Subtracted spectra were not normalized before subtraction.

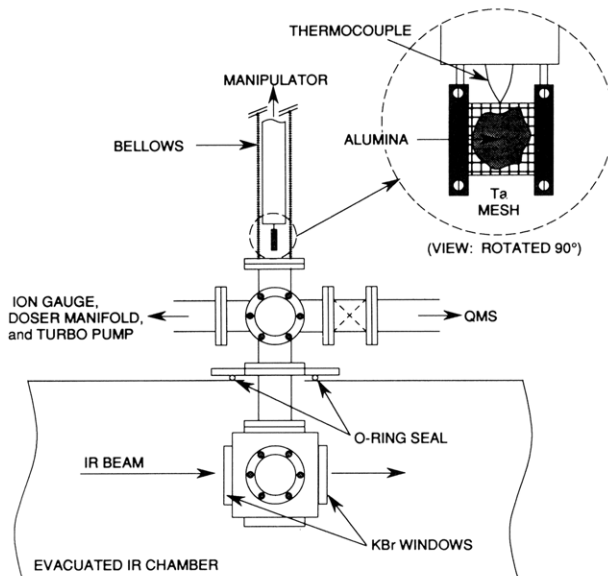


Figure 1. Schematic diagram of the experimental apparatus.

The γ -alumina substrate for all experiments was aluminum oxide C (Degussa AG, Frankfurt, FRG) with an as-received surface area of $100\text{ m}^2/\text{g}$ and an average particle diameter of 20 nm . A new sample was prepared for each set of experiments by hand pressing the alumina powder into a tantalum mesh; the alumina was mounted as-received. The mesh was clamped between two stainless steel arms connected to power feedthroughs, such that the mesh served as a resistive heating element. A chromel–alumel thermocouple was spot welded to the top center portion of the mesh to monitor temperature. For TPD, the surface temperature was controlled by a temperature controller (Eurotherm, Co., Model 906, West Sussex, UK) which linearly ramped the surface temperature at 5 K/s . The temperature controller and a quadrupole mass spectrometer (Model 100C, UTI Instrument, Co., Milpitas, CA) were interfaced to a computer for data acquisition. The TPD system was capable of monitoring up to 10 atomic masses simultaneously. Prior to all experiments, the alumina was heated at 420 K overnight in vacuum, yielding a hydroxylated surface.¹

Semiconductor-grade TMAI (Akzo Chemicals, Inc., Deer Park, TX) was purified before each set of experiments by freezing the bubbler in liquid nitrogen and pumping away the volatile impurities. Both FTIR³⁵ and mass spectra of gas-phase TMAI agreed well with published data. No impurities were evident with the exception of methane produced from reactions of TMAI with the chamber walls and filaments. Anhydrous ammonia (Matheson Gas Products, Secaucus, NJ) was used without further purification. IR³⁶ and mass spectra of the NH_3 were in agreement with well-known standards, and no impurities were detected. Exposures were achieved in a static mode with all exposures reported in langmuirs ($1\text{ langmuir} = 10^{-6}\text{ Torr s}$).

Samples were removed from the FTIR/TPD apparatus and transferred to an S-Probe ESCA Console (Surface Science Instruments, Inc., Mountain View, CA) for XPS measurements. The system was equipped with a monochromatized Al anode X-ray source and a hemispherical electron energy analyzer coupled to a multichannel detector. Measurements were taken at a pass energy of 150 eV , a beam spot size of $0.25 \times 1\text{ mm}^2$, and with a low-energy electron flood gun to neutralize surface charging. The peak positions were calibrated using the hydrocarbon peak referenced to 285.0 eV . The powders were mounted by pressing them into indium foil which was mounted with double-sided cellophane tape to the XPS sample chuck such that the samples were electrically floating.

(33) Kodama, K.; Ozeki, M.; Mochizuki, K.; Ohtsuka, N. *Appl. Phys. Lett.* 1989, 54, 656.

(34) Yu, M. L.; Memmert, U.; Kuech, T. F. *Appl. Phys. Lett.* 1989, 55, 1011.

(35) Kvisle, S.; Rytter, E. *Spectrochim. Acta* 1984, 40A, 939.

(36) *Standard IR Grating Spectra*; Sadtler Research Laboratories, Inc., Philadelphia, 1974.

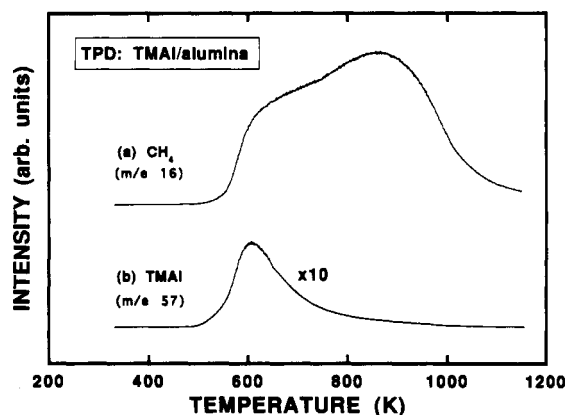


Figure 2. TPD spectra of (a) m/e 16 (methane) and (b) m/e 57 (TMAI) following (a) of 2×10^8 -langmuir saturation exposure of TMAI to an alumina substrate held at 500 K.

Results and Discussion

In previous work¹ we have determined that when TMAI is reacted with an alumina powder surface from 300 to 500 K, the dominant surface species formed is dimethyl-alumino (Me_2Al) singly bound to oxygen. To investigate the thermal stability of this species, we carried out thermal desorption experiments, in which an exposure of 2×10^8 langmuirs of TMAI was applied to an alumina substrate held at 500 K, followed by ramping the temperature from 300 to 1150 K, while monitoring appropriate atomic masses with the quadrupole mass spectrometer. Shown in Figure 2 is a plot of the m/e 16 (methane) and m/e 57 intensities versus temperature. The m/e 57 is the dominant peak in the cracking pattern of TMAI. The Me_2Al is stable to about 550 K, at which point it begins to decompose liberating methane as the predominant product over a broad temperature range from 550 to 1000 K. There is also a small amount of TMAI desorption (m/e 57) which begins to desorb at the same temperature that methane desorption commences, has a peak temperature of ~ 600 K, and has a long tail to temperatures >1000 K. Other masses characteristic of methane and TMAI desorption were also monitored and showed identical line shapes to those presented in the figure.

On the basis of previous studies,^{1,2} we believe that the hydrogen which combines with the $-\text{CH}_3$ to form methane comes from the thermal decomposition of some of the Me_2Al - species during TPD. We see no evidence for hydrogen adsorbed to aluminum in the IR data (Al-H stretch $\sim 1800 \text{ cm}^{-1}$) prior to TPD. However, with our experimental arrangement, we cannot unambiguously rule out other sources, such as small concentrations of hydrogen present in hydroxyl groups on the alumina substrate or hydrogen from reaction with the walls of the chamber.

When the Me_2Al surface species is subsequently exposed to NH_3 at room temperature, FTIR data¹ have shown that a weakly bound $\text{Me}_2\text{Al}:\text{NH}_3$ adduct is formed, along with amide ($-\text{NH}_2-$) bridge-bonded to aluminum. We were also interested in the thermal stability of these species and shown in Figure 3 is the thermal desorption spectrum taken after a saturation exposure of TMAI (2×10^8 langmuirs at 500 K) followed by a 10^9 -langmuir NH_3 saturation exposure applied at room temperature. The methane signal at m/e 16 exhibits the same behavior as the case when TMAI was dosed alone, except for an additional low-intensity tail in the temperature range 400–550 K. The source of this additional m/e 16 signal is

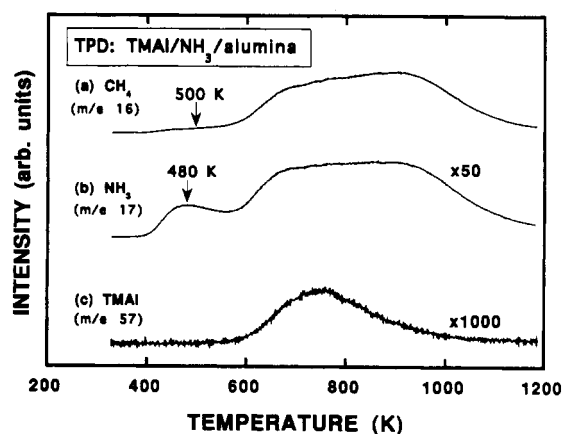


Figure 3. TPD spectra of (a) m/e 16 (methane), (b) m/e 17 (NH_3), and (c) m/e 57 (TMAI) following sequential saturation exposures of TMAI (2×10^8 langmuirs) and NH_3 (10^9 langmuirs) to alumina. The alumina was held at 500 K for the TMAI exposure and 300 K for the NH_3 exposure.

methane released as the NH_3 adduct reacts with Me_2Al to form additional $-\text{NH}_2-$. This observation is consistent with the FTIR data reported previously,¹ in which the integrated area of the $-\text{NH}_2-$ bend peak (at 1513 cm^{-1}) increased by 20% when heated in the range of 500 to 600 K.

For m/e 17 (NH_3), there is a peak centered at a temperature ~ 480 K, which is assigned to the dissociation of the weakly bound NH_3 adduct. This result also agrees with previous FTIR data,¹ in which the antisymmetric NH_3 bend peak (1620 cm^{-1}) intensity dropped by roughly a factor of 2 as the surface temperature was raised to 470 K and was almost completely gone by 600 K. The remainder of the m/e 17 signal above ~ 600 K is the naturally abundant carbon-13 fraction from the methane desorption ($^{13}\text{CH}_4$).

Finally, TMAI (m/e 57) desorption exhibits a single broad peak in the temperature range 600 to >1000 K with a peak maximum at ~ 750 K. The amount of TMAI desorption has been greatly reduced by the presence of NH_3 compared to case of TMAI exposure alone, and the temperature of the peak maximum shifts to higher temperature. The temperature range of this desorption feature is in good agreement with the high-temperature tail from Figure 2b where TMAI was dosed alone. In both cases, the desorption in this temperature range probably arises from thermal decomposition of isolated MeAl or Me_2Al groups and subsequent surface reactions to form TMAI which then desorbs at these temperatures.

The conversion of the $\text{Me}_2\text{Al}:\text{NH}_3$ adduct and a neighboring Me_2Al group to the bridge-bonded $-\text{NH}_2-$ at elevated temperature appears to be limited by a competing reaction, namely, the desorption of the weakly bound NH_3 from the adduct. As the temperature is raised, the rate of the $-\text{NH}_2-$ forming reaction increases, but at the same time the NH_3 available for reaction is quickly depleted. To counteract the NH_3 lost by desorption, we dosed NH_3 at elevated temperature to ensure that a constant supply was available for reaction. Shown in Figure 4 are FTIR spectra after a saturation exposure of TMAI at 500 K, curve (a), and a subsequent saturation exposure of NH_3 at 600 K, curve (b). For comparison, Figure 4c is the FTIR spectrum after a saturation dose of TMAI at 500 K, followed by a saturation dose of NH_3 at 300 K. The spectra were normalized such that the methyl bend and stretch

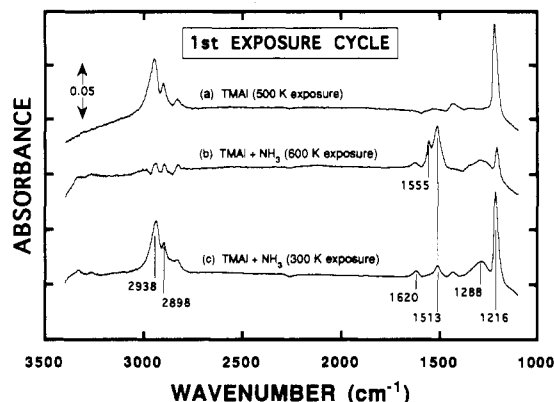


Figure 4. FTIR spectra following (a) saturation exposure of TMAI to alumina held at 500 K, (b) subsequent saturation exposure of NH_3 at 600 K, and (c) after saturation exposures of TMAI at 500 K followed by NH_3 at 300 K.

features observed after TMAI saturation but prior to NH_3 exposure had the same peak area. For reference in Figure 4c, peaks of interest include antisymmetric and symmetric $-\text{CH}_3$ stretching modes at 2938 and 2898 cm^{-1} , respectively, symmetric $-\text{CH}_3$ bending modes at 1216 cm^{-1} , antisymmetric $-\text{NH}_3$ bending modes at 1620 cm^{-1} , symmetric $-\text{NH}_3$ bending modes at 1288 cm^{-1} (four-coordinate nitrogen), and $-\text{NH}_2$ bending modes at 1513 cm^{-1} (four-coordinate nitrogen).

It is apparent from Figure 4 that the reaction efficiency to form $-\text{NH}_2$ has dramatically increased when the NH_3 is dosed at 600 K. In the case of room temperature dosing (Figure 4c), the $-\text{NH}_2$ feature at 1513 cm^{-1} is small compared to the methyl-related features, which did not lose appreciable intensity after NH_3 exposure. On the other hand, for the case at 600 K (Figure 4b), the $-\text{NH}_2$ feature is now much more intense than the methyl features, which have been reduced by a factor of ~ 4.5 (based on the symmetric $-\text{CH}_3$ bend peak area) from the loss of methyl groups as methane. The integrated peak area of the $-\text{NH}_2$ bend is about 4 times larger for 600 K dosing compared to 300 K NH_3 dosing. An additional peak at 1555 cm^{-1} has also appeared, which is assigned to the bending mode of $-\text{NH}_2$ with three-coordinate nitrogen.³⁷

Upon close examination of the $-\text{CH}_3$ symmetric bend peak at $\sim 1216 \text{ cm}^{-1}$ in Figure 4a, we find it consists of two components corresponding to the A_1 (in-phase) and B_1 (out-of-phase) representations, at 1223 and 1214 cm^{-1} , respectively, leading to an asymmetric line shape and consistent with what we have reported previously.¹ After the exposure of NH_3 at 600 K, however, the peak position drops to 1207 cm^{-1} , and the line shape changes and becomes almost perfectly symmetric. This behavior is illustrated in the inset of Figure 5 where the $-\text{CH}_3$ symmetric bend for alumina saturated with TMAI is shown at higher resolution before and after reaction with NH_3 . For a monomethylaluminum (MeAl) surface complex, only a single symmetric $-\text{CH}_3$ bending mode is active. Thus, we believe this change in line shape is a result of the majority of the Me_2Al reacting with the NH_3 to leave MeAl on the surface. In addition, aluminum with no methyl groups attached are probably present on the surface but cannot be detected with IR in this wavenumber range. This picture is consistent with the increased quantity of $-\text{NH}_2$ which is formed when NH_3 is dosed at 600 K.

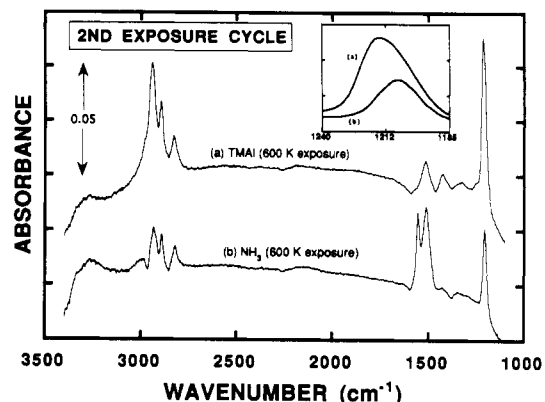


Figure 5. FTIR spectra for a second exposure cycle with the alumina held at 600 K; (a) after TMAI saturation, and (b) after NH_3 saturation. Inset: the $-\text{CH}_3$ symmetric bend peak with the abscissa expanded.

The thermal desorption results given above show that the Me_2Al begins to thermally decompose at about 550 K. To ensure that the decrease in methyl group population observed in Figure 4b was a result of NH_3 reacting to form $-\text{NH}_2$ and not simply thermal breakdown of Me_2Al , we heated the TMAI saturated surface (Figure 4a) to 600 K for 1 min (which is comparable to the NH_3 dosing time at 600 K). After this treatment the integrated intensity of the methyl group IR peaks decreased only by about 15% compared to the factor of 4.5 decrease shown in Figure 4b where NH_3 is present, indicating that it is indeed the $-\text{NH}_2$ -forming reaction that is responsible for the majority of the loss of methyl groups. In subsequent experiments, we dosed TMAI at 600 K, and observed no significant differences in the IR spectra, compared to dosing at 500 K. Most significantly, at 600 K (as was found at 500 K) the symmetric $-\text{CH}_3$ bend peak exhibits the line shape characteristic of the presence of two modes, suggesting that the majority species is Me_2Al .

We cannot determine from our data the detailed mechanistic of the CH_4 elimination reaction. That is, we cannot distinguish whether a CH_3 group is eliminated, combines with a surface hydrogen from an NH_3 group and desorbs as CH_4 , or whether a hydrogen from a neighboring adduct assists in the C-Al bond scission leading directly to CH_4 elimination. Both mechanisms lead to CH_4 desorption which is detected in the TPD experiment. The latter mechanism has been suggested for a similar reaction on a silica surface where isotopic labeling was used to help elucidate the mechanism.^{3,38}

We also wanted to verify that it was specifically the interaction of the Me_2Al with the NH_3 which lead to the enhanced formation of $-\text{NH}_2$ at 600 K. To this end, we saturated a clean alumina substrate held at 600 K with NH_3 (10^9 -langmuir exposure). A relatively small $-\text{NH}_2$ peak did appear, but its intensity was at least 6.5 times smaller than the case with Me_2Al present. In addition, based on the antisymmetric $-\text{NH}_3$ bend peak area at $\sim 1620 \text{ cm}^{-1}$, the $-\text{NH}_3$ population was about a factor of 12 larger on the clean alumina than on Me_2Al -saturated alumina. (Note that NH_3 will begin desorbing from alumina near 600 K,¹ but substantial amounts are still present after dosing under these conditions and rapidly reducing the surface temperature to obtain the IR data.) These results

(37) Morrow, B. A.; Cody, I. A.; Lee, L. S. M. *J. Phys. Chem.* 1976, 80, 2761.

(38) Bartram, M. E.; Michalske, T. A.; Rogers, Jr., J. W.; Paine, R. T. *Chem. Mater.* 1993, 5, 1424.

confirm that it is the presence of the Me_2Al which is dominating the surface chemistry at 600 K.

To achieve growth of useful epitaxial layers by alternate exposure of group III and V precursors (atomic layer growth), many exposure cycles are required, which in turn requires selective adsorption and facile reaction of both species. To investigate this potential, we performed multiple cyclic exposures of TMAI and NH_3 , both dosed at 600 K. Shown in Figure 5 are FTIR spectra for the second in a series of such cycles. Curve (a) was obtained after TMAI saturation and curve (b) after subsequent NH_3 saturation. (Note that this is a continuation of the first cycle shown in Figure 4a,b.) In Figure 5a, we find that the typical methyl-related peaks are present with roughly the same intensity as for the original TMAI saturation shown in Figure 4a, and the symmetric $-\text{CH}_3$ bend peak centered at 1215 cm^{-1} has regained the two components indicative of Me_2Al . Concurrently, the $-\text{NH}_2$ population has been reduced by about a factor of 3, signifying that the TMAI has reacted selectively with the nitrogen sites on the surface.

Subsequent exposure of NH_3 at 600 K (Figure 5b) leads to a reduction of the methyl group population by about a factor of 2.5, again with the symmetric $-\text{CH}_3$ bend peak shifting down to 1207 cm^{-1} , and acquiring the symmetric line shape indicative of MeAl (see inset). Meanwhile, the $-\text{NH}_2$ bend peak has regained intensity roughly equal to that present after the first NH_3 exposure shown in Figure 4b. The peak corresponding to three-coordinate $-\text{NH}_2$ at 1555 cm^{-1} has also reappeared. The entire spectrum after the second complete TMAI/ NH_3 cycle (Figure 5b) is effectively the same as after the first cycle (Figure 4b), with the exception that the features corresponding to NH_3 (~ 1620 and $\sim 1288\text{ cm}^{-1}$) are not present after the second cycle. Finally, a third exposure cycle was carried out at 600 K, and the FTIR spectra were essentially identical to those shown in Figure 5a,b. Thus, for cyclic deposition at 600 K, we have site-selective adsorption of the TMAI, followed by facile reaction with NH_3 to create new sites for TMAI adsorption/reaction.

Unfortunately, we do not have a direct IR fingerprint for AlN in the wavenumber range studied. The Al-N stretching mode in AlN ($\sim 670\text{ cm}^{-1}$) occurs in a wavenumber range at which the alumina substrate absorbs virtually all of the IR signal. To verify the presence of AlN after processing, XPS experiments were carried out. After the third deposition cycle was completed as described above, and following TPD in which the sample temperature was ramped to 1100 K, the sample was removed from vacuum and transferred to a separate high-vacuum chamber equipped with XPS. Shown in Figure 6 is the $\text{N}(1s)$ region. Curve-fitting reveals two peaks with binding energies centered at 397.2 and 399.9 eV. The peak at 399.9 eV is assigned to NH_2 , based on data obtained from silicon³⁹ and metal⁴⁰ substrates. The presence of NH_2 in the XPS is in agreement with the IR results which indicate that four-coordinate NH_2 (1513 cm^{-1}) is still present at the end of a reaction cycle and after annealing to 1100 K. The larger intensity peak at 397.2 eV closely matches those observed in AlN ⁴¹⁻⁴³ indicating the formation of AlN on the surface. Thus, these results are in complete agreement

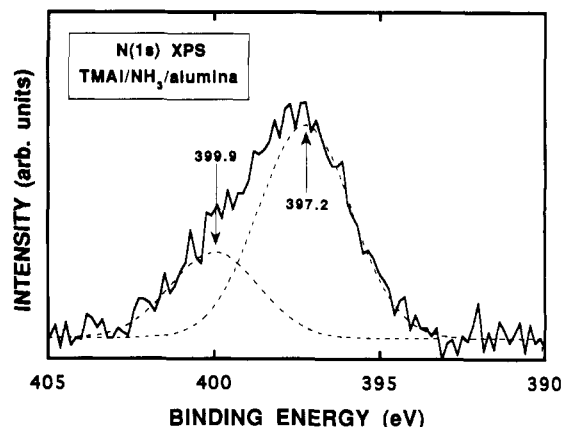


Figure 6. XPS of the $\text{N}(1s)$ region following three sequential dosing cycles of TMAI/ NH_3 with the alumina held at 600 K.

with the IR and TPD results reported above. By comparison, no nitrogen signal was detected at all on alumina after one exposure cycle of TMAI and NH_3 at 300 K followed by a 1200 K anneal.

Additional XPS experiments (not shown) were performed in a different chamber in which data could be obtained immediately after TMAI and NH_3 dosing at 600 K. A nitride peak was also observed under those conditions although it was not the dominant species. Those results will be presented in a subsequent publication.

Conclusions

In summary, TMAI reacts on a γ -alumina powder surface in the temperature range from 300 to 600 K to form a dimethylaluminum (Me_2Al) surface complex. This complex begins to decompose above 550 K, liberating methane gas and a small amount of TMAI. NH_3 reacts with a TMAI-saturated alumina surface at room temperature to form four-coordinate, $-\text{NH}_2$ bridge-bonded to Al, as well as a $\text{Me}_2\text{Al}:\text{NH}_3$ adduct. As the temperature is raised above 500 K the adduct either decomposes to liberate NH_3 gas or reacts with Me_2Al to form more bridge-bonded $-\text{NH}_2$. This reaction to form $-\text{NH}_2$, i.e., extended covalently bonded Al-N networks, is limited at elevated temperatures by the thermal desorption and depletion of NH_3 . When NH_3 is dosed to an alumina substrate held at 600 K as opposed to room temperature, the $-\text{NH}_2$ -forming reaction efficiency is greatly enhanced, as evidenced by a 4-fold increase in the $-\text{NH}_2$ -bending mode intensity, accompanied by about a 4.5 times reduction in methyl group population. In addition, changes in the line shape of the symmetric $-\text{CH}_3$ bend peak shows that Me_2Al is converted to MeAl upon exposure of NH_3 at 600 K. Repeated cyclic processing at 600 K leads to site-selective adsorption of the group III species, followed by facile reaction with the group V species to create new sites for the group III reaction, i.e., atomic layer growth. Finally, XPS data confirm that AlN is formed after three TMAI/ NH_3 exposure cycles at 600 K.

Acknowledgment. The authors gratefully acknowledge support for this work by the National Science Foundation under grant CTS-9303974, Pacific Northwest Laboratories, and the Washington Technology Center.

(39) Bischoff, J. L.; Lutz, F.; Bolmont, D.; Kubler, L. *Surf. Sci.* **1991**, *251*, 170.

(40) Schreifels, J. A.; Deffeyes, J. E.; Neff, L. D.; White, J. M. *J. Electron Spectrosc. Relat. Phenom.* **1982**, *25*, 191.

(41) Baier, H.; Monch, W. *J. Appl. Phys.* **1990**, *68*, 586.

(42) Gautier, M.; Duraud, J. P.; Greussus, C. *Le J. Appl. Phys.* **1987**, *61*, 574.

(43) Kovacich, J. A.; Kasperkiewicz, J.; Lichtman, D.; Aita, C. R. *J. Appl. Phys.* **1984**, *55*, 2935.